Adaptive Fuzzy Iterative Learning Control for High-Speed Trains With Both Randomly Varying Operation Lengths and System Constraints

Qiongxia Yu and Zhongsheng Hou, *Fellow, IEEE*

***Abstract*—In this article, a new adaptive fuzzy iterative learning control (AFILC) method is proposed for the tracking control of nonlinear uncertain high-speed train (HST) operation systems that have both randomly varying iteration lengths and speed and input force constraints. To cope with unknown time-varying basic resistance coefficients, an adaptive learning control law and two fully projected parameter learning laws are designed. The nonparametric and unknown additional resistance in the HST operation system is compensated and integrated into the control law by means of a newly constructed adaptive iterative learning fuzzy system. Moreover, due to the complex operation environment and various uncertainties, disturbances and emergencies, trains are often early or late compared with the prearranged timetable rather than being strictly on time in the repeated operations of each day, which leads to randomly varying operation lengths for actual HST running. Furthermore, as the traveling speed of modern HSTs increases, both the train's speed and input force should be constrained to guarantee the safe operation. Fortunately, the proposed AFILC can not only actively manipulate the position, speed, and input force of the train into prespecified and constrained ranges for safe operation but can also make both the position and speed tracking control errors converge to zero over the whole desired and scheduled time interval, even if the actual time interval varies in each operation of the HST. Simulations on a practical train operation system similar to China Railway High-speed (CRH)-3 train are further presented to demonstrate the applicability and effectiveness of the proposed method.**

***Index Terms*—Adaptive iterative learning control, fuzzy iterative learning control, system constraints, varying iteration length.**

I. Introduction

As a fast, comfortable, energy-saving, high-loading capacity and environmentally friendly transportation system, high-speed trains (HSTs) are becoming increasingly popular with modern people. In practice, HST operation systems are characterized by prominent operating features, including as follows:

1) Everyday, an HST repeatedly executes the same passenger transportation task in the same fixed time interval.
2) The nonlinear HST has both parametric and nonparametric system uncertainties.
3) In practical operation of the HST, due to the complex operation environment and various uncertainties and emergencies, a train often randomly reaches the terminus early or late in each operation/iteration rather than being strictly on time.
4) To protect the HST from over speed and actuator saturation, the operating speed and input force of the train must be constrained.

Iterative learning control (ILC) is an ideal control method to address the control problem of a system repeated over a finite time interval [1]. In fact, if the operating time interval of the HST does not vary each day, namely, the iteration length of the HST operation system is the same everyday, by learning control information from preceding operations, for each time point, ILC can make the actual position and speed of the HST match the desired position and speed trajectories perfectly. By contrast, the existing time-domain control methods for HSTs [2]–[10] can cause the actual errors in the position and speed of the HST to converge only when the time index goes to infinity, which is not suitable for the systems that operate repeatedly over a finite time interval. Moreover, the transient behavior, especially in the initial operating stage, may not be improved no matter how many times the system repeats. Therefore, compared with the time-domain control methods, ILC is more suitable for the control of HST operation systems.

To cope with the time-varying even fast time-varying parametric uncertainties in HST operation systems, some works on adaptive ILC have recently been proposed [11]–[14]. Li and Hou [11] designed an adaptive ILC for HSTs with measurement noise; Yu *et al.* [12] proposed an adaptive ILC with both state and input constraints that is simulated based on a HST. However, the complex additional resistance in these two works is considered

Manuscript received November 19, 2019; revised April 1, 2020; accepted May 28, 2020. Date of publication June 4, 2020; date of current version August 4, 2021. This work was supported in part by the National Natural Science Foundation of China under Grant 61833001, Grant 61433002, Grant 61573129, and U1804147, in part by the Ph.D. Programs Foundation of Henan Polytechnic University under Grant B2018-28, in part by the Fundamental Research Funds for the Universities of Henan Province under Grant NSFRF200324, in part by the Beijing Natural Science Foundation under Grant L161007, in part by the Innovative Scientists and Technicians Team of Henan Provincial High Education under Grant 20IRTSTHN019, and in part by the Innovative Scientists and Technicians Team of Henan Polytechnic University under Grant T2019-2. *(Corresponding author: Qiongxia Yu.)*

Qiongxia Yu is with the School of Electrical Engineering and Automation, Henan Polytechnic University, Jiaozuo 454000, China (e-mail: qiongxiayu@hotmail.com).

Zhongsheng Hou is with the School of Automation, Qingdao University, Qingdao 266071, China (e-mail: zhshhou@bjtu.edu.cn).

Color versions of one or more of the figures in this article are available online at https://ieeexplore.ieee.org.

Digital Object Identifier 10.1109/TFUZZ.2020.2999958

as an unknown time-varying parameter. Ji *et al.* [13], [14] considered the unknown additional resistance as parametric uncertainty and proposes an adaptive ILC with unknown speed delays and input saturations for HSTs. In reality, the additional resistance is related to the position of the train and varies from operation to operation based on the different running times, complex operation environment, and various uncertainties [15], [16] such that it is more reasonable to be considered as nonparametric uncertainty. In this article, a new adaptive iterative learning fuzzy system is constructed to describe and compensate the unknown and nonparametric additional resistance for the first time.

More importantly, in the existing works that apply the aforementioned adaptive ILC for HSTs [11]–[14] or other types of ILC methods for HSTs [17], [18], a common assumption is that the time interval of the train's operation everyday is strictly same constant. However, in fact, in each day's operation, a train is always early or late rather than on time compared with its timetable owing to various uncertainties and randomly occurring events. Until now, no work has applied adaptive ILC with varying iteration lengths for HSTs, and there is only one piece of work in Yu *et al.* [19] that applied the traditional P-type ILC with varying trial lengths for the HST operation system. Actually, in the field of ILC, researchers have focused on some different types of ILC methods with varying iteration lengths for different control systems [20]–[25]. Li *et al.*, Shen *et al.*, and Shi *et al.* [20]–[23] addressed a series of iteration-average operator based traditional ILC methods with randomly varying iteration lengths for discrete-time linear systems [20]–[22] and nonlinear stochastic systems [23]. In Bu *et al.* [24] and Shen and Xu [25], discrete-time model-free adaptive ILC and continuous-time adaptive ILC are proposed, respectively, for a class of nonlinear systems with randomly varying iteration lengths.

Notably, in these aforementioned works for the problem of varying iteration lengths [19]–[25], the issue of randomly varying trial lengths is addressed for the considered linear or nonlinear system only, while any constraints on state or input are not embraced for the considered systems. Since the input and state constraints are vital for the safe operation of the HST, it is of great significance to design an ILC method for HST operation systems under both randomly varying iteration lengths and system constraints.

Motivated by the above discussion, a new adaptive fuzzy ILC (AFILC) is proposed in this article for nonlinear HST operation systems with both parametric and nonparametric system uncertainties, randomly varying iteration lengths, and system constraints. The contributions of this article are as follows.

1) In the last few years, fuzzy systems have achieved significant developments in both theory [26]–[31] and applications [32]–[34]. In contrast with these existing fuzzy modeling and control methods in the time domain [26]–[34] that guarantee asymptotic convergence of the control errors, which implies that zero control errors are achieved only as the operation time of the system approaches infinity, the proposed adaptive fuzzy ILC can make the control error of each time point in the whole finite and desired operating time interval converge to zero, even if the operation lengths for each run of the system are randomly varying.
2) In contrast with the existing methods for HSTs in both iteration-domain [11]–[14], [17], [18] and time-domain [2]–[10], the proposed new AFILC can address nonparametric uncertainties in the HST by means of a novel constructed adaptive iterative learning fuzzy system and can automatically regulate both speed and input force signals of the HST into the constrained ranges, while simultaneously handling randomly varying operation lengths.
3) In contrast with the existing methods that deal with the varying iteration lengths [19]–[25], by incorporating a barrier composite energy function (BCEF) into the controller, the proposed new AFILC can overcome the problems of randomly varying iteration lengths and system constraints simultaneously for a class of repetitive nonlinear systems with nonparametric uncertainties.

The rest of this article is organized as follows. Section II gives the model description and operational characteristics of HSTs. Section III presents the proposed AFILC and a convergence analysis. Section IV provides simulation results on the CRH-3 HST operation systems. Finally, Section V concludes this article.

II. Problem Formulation

A. Model Description of a HST

By Newtonian law, the dynamic model of a HST can be described as [15], [16]:

$$\begin{aligned}\dot{s}_k(t) &= v_k(t)\\ \dot{v}_k(t) &= F_k(t) - f_b(v_k(t)) - f_a(s_k(t)) + d_k(t)\end{aligned} \tag{1}$$

where subscript $k \in \mathbf{Z}_+$ represents the iteration index and $t \in [0, T_k]$ (s) represents the continuous-time index. $s_k(t)$ (m) and $v_k(t)$ (m/s) denote the operating position and speed of the HST, respectively. The control input $F_k(t)$ (N/kg) denotes traction force (or braking force when negative) on a unit mass. $f_b(v_k(t))$ (N/kg) is the basic resistance on a unit mass. $f_a(s_k(t))$ (N/kg) is the additional resistance on a unit mass that exists in special sections such as curves, ramps, and tunnels. $d_k(t)$ (N/kg) represents unknown external disturbances on a unit mass.

Remark 1: A common assumption in the existing works on the application of ILC to train operation control is that the train should operate strictly within the fixed time interval $[0, \mathtt{T}]$ for each repeated operation. Actually, due to various uncertain factors and external disturbances, a train may arrive at the station earlier or later than scheduled such that the actual operating time interval $[0, T_k]$ may vary as the operating number k varies. In particular, if the train arrives early, that is, $T_k < \mathtt{T}$, the system will produce incomplete data information in the time interval $[T_k, \mathtt{T}]$ such that there will be no effective operation data to update the control input of the next operation. This is a challenge for designing appropriate traction or braking force to guarantee effective and safe operation of the HST.

With regard to the dynamics of the considered HST operation system (1), the following assumptions are made.

Assumption 1: Denote a state vector of the train as $\boldsymbol{x}_k(t) = [s_k(t), v_k(t)]^T$ and a desired state vector as $\boldsymbol{p}(t) = [p_1(t), p_2(t)]^T$. Then, the identical initial condition is satisfied, namely $p_1(0) - s_k(0) = 0, p_2(0) - v_k(0) = 0 \; \forall k \in \mathbf{Z}_+$.

Assumption 2: The desired state vector $\boldsymbol{p}(t)$ and its first time-derivative $\dot{\boldsymbol{p}}(t)$, as well as the unknown and time-iteration-varying external disturbances $d_k(t)$ are all bounded $\forall t \in [0, \mathtt{T}]$ and $\forall k \in \mathbf{Z}_+$.

Remark 2: Assumption 1 implies that the train runs from the departure station with the same starting position and speed every day and is reasonable for practical operation of the train. In fact, it is a common assumption in the context of ILC and can be easily relaxed, as has been done in our previous work [12]. Assumption 2 is a common assumption for practical control systems.

Then, the basic resistance $f_b(v_k(t))$ and the additional resistance $f_a(s_k(t))$ are specified as follows.

The basic resistance $f_b(v_k(t))$ can be described as [15], [16]

$$f_b(v_k(t)) = a(t) + b(t)v_k(t) + c(t)v_k^2(t) \tag{2}$$

where $a(t) + b(t)v_k(t)$ is the mechanical resistance and $c(t)v_k^2(t)$ is the aerodynamic resistance [35]. $a(t)$, $b(t)$, and $c(t)$ are time-varying or even fast time-varying and completely unknown basic resistance coefficients.

The additional resistance $f_a(s_k(t))$ is associated with the position of the train. Although the train runs in a known dedicated line, the train is not guaranteed to reach the same ramp, curve, or tunnel at the same time in each repeated operation due to the complex operation environment and various uncertainties. Therefore, $f_a(s_k(t))$ is an unknown nonlinear function described by the following iterative learning fuzzy system.

$f_a(s_k(t))$ can be modeled by a collection of fuzzy IF–THEN rules as follows:

$$R^l: \text{ if } s_k(t) \text{ is } A_1^l, \text{ and } v_k(t) \text{ is } A_2^l \text{ then}$$
$$\hat{f}_a^l(s_k(t)) \text{ is } w^l(t), \quad l = 1, 2, \ldots, N \tag{3}$$

where R^l is the lth rule and N is the total number of rules that describes the unknown additional resistance. $s_k(t)$ and $v_k(t)$ are the inputs of the fuzzy system, and $\hat{f}_a(s_k(t))$, which is the estimate of the unknown $f_a(s_k(t))$, is the output of the fuzzy system. The linguistic terms A_1^l and A_2^l are characterized by the fuzzy membership functions $\mu_{A_1^l}(s_k(t))$ and $\mu_{A_2^l}(v_k(t))$, which are defined as the following Gaussian functions:

$$\mu_{A_1^l}(s_k(t)) = e^{-\frac{\left(s_k(t) - m_1^l(t)\right)^2}{2\sigma_1^l(t)^2}} \tag{4}$$

and

$$\mu_{A_2^l}(v_k(t)) = e^{-\frac{\left(v_k(t) - m_2^l(t)\right)^2}{2\sigma_2^l(t)^2}} \tag{5}$$

where $m_j^l(t)$ and $\sigma_j^l(t)$, $j = 1, 2$ are the center and width of the membership function, respectively. Then, the output of the fuzzy system can be expressed as

$$\hat{f}_a(s_k(t)) = \frac{\sum_{l=1}^N w^l(t)\mu_{A_1^l}(s_k(t))\,\mu_{A_2^l}(v_k(t))}{\sum_{l=1}^N \mu_{A_1^l}(s_k(t))\,\mu_{A_2^l}(v_k(t))}. \tag{6}$$

Let

$$\delta^l(s_k(t), v_k(t), t) = \frac{\mu_{A_1^l}(s_k(t))\,\mu_{A_2^l}(v_k(t))}{\sum_{l=1}^N \mu_{A_1^l}(s_k(t))\,\mu_{A_2^l}(v_k(t))}. \tag{7}$$

Then, (6) can be rewritten as

$$\hat{f}_a(s_k(t)) = \sum_{l=1}^N w^l(t)\delta^l(s_k(t), v_k(t), t). \tag{8}$$

Wang [36] had shown that the function approximation error between the output of the fuzzy system $\hat{f}_a(s_k(t))$ and the unknown function $f_a(s_k(t))$ is bounded by a prescribed constant ε^* on a compact set Ω, that is,

$$f_a(s_k(t)) = \hat{f}_a(s_k(t)) + \varepsilon_k(t) \tag{9}$$

where the approximation error $\varepsilon_k(t)$ satisfies $|\varepsilon_k(t)| \le \varepsilon^*$.

Based on (2) and (8)–(9), (1) can be rewritten as

$$\dot{s}_k(t) = v_k(t)$$
$$\dot{v}_k(t) = F_k(t) + \boldsymbol{\theta}^T(t)\boldsymbol{\xi}(\boldsymbol{x}_k(t)) - \varepsilon_k(t) + d_k(t) \tag{10}$$

where the operating time $t \in [0, T_k]$ (s) that may vary as the operating number k varies. $\boldsymbol{x}_k(t) = [s_k(t), v_k(t)]^T$ represents the state vector of the system. $\boldsymbol{\theta}(t) = [a(t), b(t), c(t), w^1(t), \ldots, w^N(t)]^T$ and $\boldsymbol{\xi}(\boldsymbol{x}_k(t)) = [-1, -v_k(t), -v_k^2(t), -\delta^1(s_k(t), v_k(t), t), \ldots, -\delta^N(s_k(t), v_k(t), t)]^T$.

Remark 3: In general, the dynamic model (10) not only can describe the considered HST operating system (1), but also can represent many other real plants such as freeway traffic flow processes [37], robot systems [38], linear motor systems [39], etc.

Remark 4: Different from the time-domain adaptive control that only constant or slowly time-varying unknown parameters can be addressed, time-varying or even fast time-varying unknown parameters $\boldsymbol{\theta}(t)$ in (10) can be addressed in this article. Although these parameters are time-varying along the time axis, for each time point over the whole operating time interval, they can be taken as constant ones along the iteration axis and will be estimated along the iteration axis by the following proposed learning law (19)–(24).

B. Operational Characteristics of HSTs

In this article, the following two operational characteristics of HSTs are considered.

1) Randomly Varying Iteration Lengths:

Different from the existing works on ILC for HSTs, where the operating time interval is assumed to be $[0, \mathtt{T}]$, which is fixed for each operation, our work enables the time interval to be randomly varying for each operation as $[0, T_k]$, where the actual operating time T_k varies with the operating number k.

2) System Constraints:

a) To avoid large control actions which may be harmful to the control apparatus, the control input force for the train should be constrained, i.e.,

$$|F_k(t)| \le F_{\max} \tag{11}$$

where $F_{\max}$ is the upper bound of $F_k(t)$.

b) To prevent a train from over speed, the operating speed of the train should be constrained, i.e.,

$$|v_k(t)| \le v_{\max} \tag{12}$$

where $v_{\max}$ is the upper bound of the operating speed $v_k(t)$.

Remark 5: With the increase of the traveling speed of modern HSTs, speed constraint is vital for safety. In practice, the automatic train protection (ATP) subsystem is in charge of protecting a train from over speed and conforming to the "fail-safe" principle. However, if a wrong command is outputted or the "fail-safe" cannot be realized upon equipment failure, the ATP

subsystem will fail to protect the train from over speed. With a view to achieve higher safety, the proposed control method in this article will provide another channel to automatically and actively regulate the speed signal of the HST into the constrained range and will work in parallel with the ATP subsystem.

C. Control Objective

Consider a desired state vector $\boldsymbol{p}(t) = [p_1(t), p_2(t)]^T$, which is bounded by

$$|p_j(t)| \le \eta_j, \quad j = 1, 2 \tag{13}$$

where η_1, η_2 are known positive constants generated by

$$\begin{aligned} \dot{p}_1(t) &= p_2(t) \\ \dot{p}_2(t) &= h(\boldsymbol{p}(t), t) \end{aligned} \tag{14}$$

where $h(\boldsymbol{p}(t), t)$ is a known and bounded vector function.

With randomly varying operation lengths of the train, the objective is to find $F_k(t)$ that makes the state of the train $\boldsymbol{x}_k(t) = [s_k(t), v_k(t)]^T$ defined in (10) track the desired state vector $\boldsymbol{p}(t)$ over the whole desired time interval $[0, \mathtt{T}]$ without violating the system constraints (11), (12), such that effective and safe operation of the HST can be achieved.

III. Adaptive Fuzzy ILC Design

Denote the state error vector $\boldsymbol{e}_k(t)$ as

$$\begin{aligned} \boldsymbol{e}_k(t) &= [e_{1,k}(t), e_{2,k}(t)]^T \\ &= \boldsymbol{p}(t) - \boldsymbol{x}_k(t) \end{aligned} \tag{15}$$

where $e_{1,k}(t) = p_1(t) - s_k(t)$ and $e_{2,k}(t) = p_2(t) - v_k(t)$. According to (10) and (14), one can obtain $[e_{1,k}(t), e_{2,k}(t)]^T = [e_{1,k}(t), \dot{e}_{1,k}(t)]^T$.

Define an extended error as

$$\begin{aligned} \varphi_k(t) &= \psi_1 e_{1,k}(t) + e_{2,k}(t) \\ &= \boldsymbol{\psi}^T \boldsymbol{e}_k(t) \end{aligned} \tag{16}$$

where $\boldsymbol{\psi} = [\psi_1, 1]^T$.

Since $\varepsilon_k(t)$, $d_k(t)$, and $h(\boldsymbol{p}(t), t)$ are all bounded, there exists an unknown positive constant ρ such that

$$|h(\boldsymbol{p}(t), t) + \varepsilon_k(t) - d_k(t)| \le \rho. \tag{17}$$

Thus, the proposed AFILC at the kth iteration is constructed as

$$\begin{aligned} F_k(t) = \beta\varphi_k(t) + \bar{\boldsymbol{\psi}}^T \boldsymbol{e}_k(t) - \hat{\boldsymbol{\theta}}_k^T(t)\boldsymbol{\xi}(\boldsymbol{x}_k(t)) \\ + \hat{\rho}_k(t)\mathrm{sgn}(\alpha_k(t)), \quad t \le T_k \end{aligned} \tag{18}$$

where

$$\hat{\boldsymbol{\theta}}_k(t) = \begin{cases} proj_\theta(\hat{\boldsymbol{\theta}}_k^*(t)), & t \le T_k \\ \hat{\boldsymbol{\theta}}_{k-1}(t), & T_k < t \le \mathtt{T} \end{cases} \tag{19}$$

$$\hat{\boldsymbol{\theta}}_k^*(t) = \hat{\boldsymbol{\theta}}_{k-1}(t) - \boldsymbol{\Gamma}\boldsymbol{\xi}(\boldsymbol{x}_k(t))\alpha_k(t) \tag{20}$$

$$\hat{\boldsymbol{\theta}}_{-1}(t) = 0 \qquad \forall t \in [0, \mathtt{T}] \tag{21}$$

and

$$\hat{\rho}_k(t) = \begin{cases} proj_\rho(\hat{\rho}_k^*(t)), & t \le T_k \\ \hat{\rho}_{k-1}(t), & T_k < t \le \mathtt{T} \end{cases} \tag{22}$$

$$\hat{\rho}_k^*(t) = \hat{\rho}_{k-1}(t) + \kappa|\alpha_k(t)| \tag{23}$$

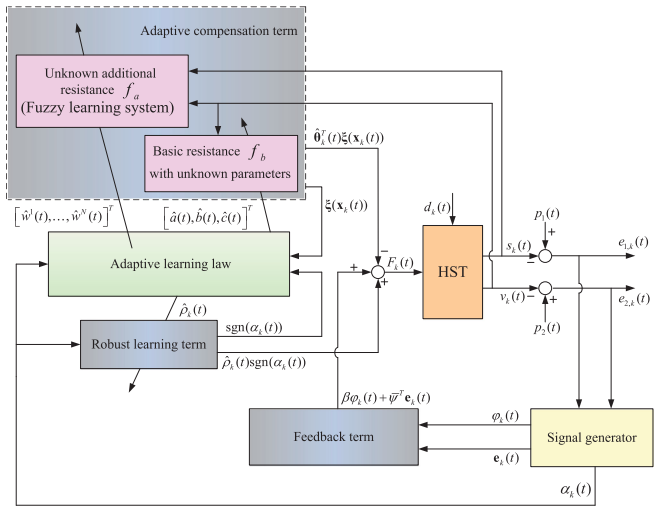

Fig. 1. Block diagram of the proposed AFILC method for the HST operation system.

$$\hat{\rho}_{-1}(t) = 0 \quad \forall t \in [0, \mathtt{T}]. \tag{24}$$

Here, $\alpha_k(t) \triangleq \frac{\varphi_k(t)}{\cos^2(\pi\varphi_k^2(t)/2k_v^2)}$. $k_v > 0$ is the constraint on $\varphi_k(t)$. $\mathrm{sgn}(\cdot)$ is the signum function, and β is a learning gain. $\bar{\boldsymbol{\psi}} = [0, \psi_1]^T$; $\hat{\boldsymbol{\theta}}_k(t) = [\hat{a}_k(t), \hat{b}_k(t), \hat{c}_k(t), \hat{w}^1(t), \ldots, \hat{w}^N(t)]^T$ and $\hat{\rho}_k(t)$ are used to learn the unknown parameter vector $\boldsymbol{\theta}(t)$ in (10) and upper bound ρ in (17). The learning gain matrix $\boldsymbol{\Gamma}$ and the learning gain κ are both positive.

Two fully projected mechanisms $proj_\theta$ and $proj_\rho$ constructed in (19) and (22) are defined as

$$proj_\theta(\hat{\boldsymbol{\theta}}_k^*(t)) = \{proj_\theta(\hat{\theta}_{j,k}^*(t))\} \quad (j = 1, \ldots, N+3)$$

$$proj_\theta(\hat{\theta}_{j,k}^*(t)) = \begin{cases} \theta_{j,\min} & \hat{\theta}_{j,k}^*(t) < \theta_{j,\min} \\ \hat{\theta}_{j,k}^*(t) & \theta_{j,\min} \le \hat{\theta}_{j,k}^*(t) \le \theta_{j,\max} \\ \theta_{j,\max} & \hat{\theta}_{j,k}^*(t) > \theta_{j,\max} \end{cases} \tag{25}$$

and

$$proj_\rho(\hat{\rho}_k^*(t)) = \begin{cases} \rho_{\min} & \hat{\rho}_k^*(t) < \rho_{\min} \\ \hat{\rho}_k^*(t) & \rho_{\min} \le \hat{\rho}_k^*(t) \le \rho_{\max} \\ \rho_{\max} & \hat{\rho}_k^*(t) > \rho_{\max} \end{cases} \tag{26}$$

where $\boldsymbol{\theta}_{\min} = [\theta_{1,\min}, \theta_{2,\min}, \ldots, \theta_{N+3,\min}]^T$ and $\boldsymbol{\theta}_{\max} = [\theta_{1,\max}, \theta_{2,\max}, \ldots, \theta_{N+3,\max}]^T$ are the minimum and maximum estimates of $\hat{\boldsymbol{\theta}}_k(t)$, and $\rho_{\min}$ and $\rho_{\max}$ are the minimum and maximum estimates of $\hat{\rho}_k(t)$, such that these estimates can be kept from diverging.

A detailed block diagram of the proposed AFILC method for the considered HST operation system (1) is presented in Fig. 1. In the diagram, the feedback term, adaptive compensation term, and robust learning term together constitute the proposed AFILC (18). The fuzzy learning system in the adaptive compensation term is constructed by (3)–(9). The adaptive learning law is implemented by (19)–(24). The signal generator formulates three error-related signals according to (15), (16) and the definition below (24), respectively.

Before giving the convergence property, the following lemma is introduced.

Lemma 1: For $\forall \boldsymbol{\theta}(t) \in [\boldsymbol{\theta}_{\min}, \boldsymbol{\theta}_{\max}]^T$ and $\rho \in \{\rho_{\min}, \rho_{\max}\}$, we have [40]

$$[\boldsymbol{\theta}(t) - proj_\theta(\hat{\boldsymbol{\theta}}_k^*(t))]^T \boldsymbol{\Gamma}^{-1} [\hat{\boldsymbol{\theta}}_k^*(t) - proj_\theta(\hat{\boldsymbol{\theta}}_k^*(t))] \leq 0 \quad (27)$$

and

$$(\rho - proj_\rho(\hat{\rho}_k^*(t)))(\hat{\rho}_k^*(t) - proj_\rho(\hat{\rho}_k^*(t))) \leq 0. \quad (28)$$

Then, the convergence of the proposed AFILC is guaranteed by Theorem 1.

Theorem 1: For the HST operation system (10) that meets Assumptions 1 and 2, the learning control law (18) and the parameter updating laws (19)–(24) guarantee that

T1) Both the position state error $e_{1,k}(t) = p_1(t) - s_k(t)$ and the speed state error $e_{2,k}(t) = p_2(t) - v_k(t)$ converge to zero asymptotically along the iteration axis $\forall t \in [0, \mathtt{T}]$, namely, $\lim_{k\to\infty} e_{i,k}(t) = 0$, $i = 1, 2$.

T2) The position, speed, and input force of the train, namely, $s_k(t)$, $v_k(t)$, and $u_k(t)$ are all bounded for any time in all iterations; meanwhile, the system constraints (11) and (12) are always obeyed.

Proof: To facilitate the analysis of the convergence property with randomly varying iteration lengths, the following auxiliary error is constructed:

$$\varsigma_k(t) = \begin{cases} \varphi_k(t), & 0 \leq t \leq T_k \\ \varphi_k(T_k), & T_k < t \leq \mathtt{T} \end{cases} \quad (29)$$

where $\varsigma_k(t) = \chi_k(t)\varphi_k(t) + (1 - \chi_k(t))\varphi_k(T_k) \quad 0 \leq t \leq \mathtt{T}$. $\chi_k(t)$ is a stochastic variable satisfying a Bernoulli distribution, i.e., $\chi_k(t) = 1$ or $\chi_k(t) = 0$. $\chi_k(t) = 1$ means that the train operation system (10) can continue to time instant t in the kth iteration.

Moreover, to illustrate the convergence property under system constraints, a positive definite barrier composite energy function (BCEF) at the kth iteration is defined as

$$\begin{aligned} J_k(t) &= \frac{k_v^2}{\pi} \tan\left(\frac{\pi \varsigma_k^2(t)}{2k_v^2}\right) + \frac{1}{2}\int_0^t \tilde{\boldsymbol{\theta}}_k{}^T(\tau)\, \boldsymbol{\Gamma}^{-1} \tilde{\boldsymbol{\theta}}_k(\tau) d\tau \\ &\quad + \frac{1}{2\kappa}\int_0^t \tilde{\rho}_k^2(\tau) d\tau \\ &\triangleq Q_k + R_k + Z_k \end{aligned} \quad (30)$$

where $Q_k \triangleq \frac{k_v^2}{\pi}\tan(\frac{\pi\varsigma_k^2(t)}{2k_v^2})$, $\tan(\cdot)$ is a tangent function, $\tilde{\boldsymbol{\theta}}_k(t) = \boldsymbol{\theta}(t) - \hat{\boldsymbol{\theta}}_k(t), \tilde{\rho}_k(t) = \rho - \hat{\rho}_k(t)$, and $R_k \triangleq \frac{1}{2}\int_0^t \tilde{\boldsymbol{\theta}}_k{}^T(\tau)\, \boldsymbol{\Gamma}^{-1}\tilde{\boldsymbol{\theta}}_k(\tau)d\tau$, $Z_k \triangleq \frac{1}{2\kappa}\int_0^t \tilde{\rho}_k^2(\tau)d\tau$.

Note that by defining the above BCEF and using the projection mechanisms (25) and (26), the proposed AFILC can actively maintain both the state and input of the train operation system in their constrained ranges. A detailed description will be shown in the following proof of T2).

Here, T1) and T2) will be proved, respectively. For notational convenience, the time index t is dropped when no confusion arises.

T1) The proof consists of two parts.

Part 1: negative definite difference of $J_k(t)$.

Determine the difference between J_k and J_{k-1},

$$\begin{aligned} \Delta J_k &= J_k - J_{k-1} \\ &= Q_k - Q_{k-1} + R_k - R_{k-1} + Z_k - Z_{k-1}. \end{aligned} \quad (31)$$

Since $\varsigma_k(t)$, $\tilde{\boldsymbol{\theta}}_k$, and $\tilde{\rho}_k(t)$ are different for $0 \leq t \leq T_k$ and $T_k < t \leq \mathtt{T}$, (31) should be analyzed for both $0 \leq t \leq T_k$ and $T_k < t \leq \mathtt{T}$.

Case 1. $t \leq T_k$: According to (29), the term Q_k in (31) becomes

$$\begin{aligned} Q_k &= \frac{k_v^2}{\pi}\tan\left(\frac{\pi\varsigma_k^2(t)}{2k_v^2}\right) = \frac{k_v^2}{\pi}\tan\left(\frac{\pi\varphi_k^2(t)}{2k_v^2}\right) \\ &= \int_0^t \frac{\varphi_k}{\cos^2\left(\frac{\pi\varphi_k^2}{2k_v^2}\right)}\dot{\varphi}_k d\tau \\ &= \int_0^t \alpha_k \dot{\varphi}_k d\tau. \end{aligned} \quad (32)$$

In terms of (16) and the definition of $\bar{\boldsymbol{\psi}}$ below (24), (32) leads to

$$Q_k = \int_0^t \left[\alpha_k(\bar{\boldsymbol{\psi}}^T \boldsymbol{e}_k + \dot{e}_{2,k})\right] d\tau. \quad (33)$$

Based on (10), (14), and (15), (33) becomes

$$\begin{aligned} Q_k &= \int_0^t \left[\alpha_k(\bar{\boldsymbol{\psi}}^T \boldsymbol{e}_k + \dot{p}_2 - \dot{x}_{2,k})\right] d\tau \\ &= \int_0^t \Big[\alpha_k(\bar{\boldsymbol{\psi}}^T \boldsymbol{e}_k + h(\boldsymbol{p}) - F_k - \boldsymbol{\theta}^T \boldsymbol{\xi}(\boldsymbol{x}_k) \\ &\quad + \varepsilon_k - d_k)\Big] d\tau. \end{aligned} \quad (34)$$

Substituting (18) into (34) yields

$$\begin{aligned} Q_k = \int_0^t \Big[\alpha_k \Big(&-\tilde{\boldsymbol{\theta}}_k^T \boldsymbol{\xi}(\boldsymbol{x}_k) - \beta\varphi_k + h(\boldsymbol{p}) \\ &+ \varepsilon_k - d_k - \hat{\rho}_k(t)\mathrm{sgn}(\alpha_k(t)))\Big] d\tau. \end{aligned} \quad (35)$$

With the definition of ρ in (17), (35) can be rewritten as

$$\begin{aligned} Q_k &\leq \int_0^t \Big[-\alpha_k \tilde{\boldsymbol{\theta}}_k^T \boldsymbol{\xi}(\boldsymbol{x}_k) - \beta\alpha_k\varphi_k \\ &\quad + |\alpha_k||h(\boldsymbol{p}) + \varepsilon_k - d_k| - |\alpha_k|\hat{\rho}_k\Big] d\tau \\ &\leq \int_0^t \left[-\alpha_k \tilde{\boldsymbol{\theta}}_k^T \boldsymbol{\xi}(\boldsymbol{x}_k) - \beta\alpha_k\varphi_k + |\alpha_k|\tilde{\rho}_k\right] d\tau. \end{aligned} \quad (36)$$

Now, let us examine the term $R_k - R_{k-1}$ in (31)

$$\begin{aligned} \tilde{R}_k &\triangleq R_k - R_{k-1} \\ &= \frac{1}{2}\int_0^t \Big[(\boldsymbol{\theta} - \hat{\boldsymbol{\theta}}_k)^T \boldsymbol{\Gamma}^{-1}(\boldsymbol{\theta} - \hat{\boldsymbol{\theta}}_k) \\ &\qquad - (\boldsymbol{\theta} - \hat{\boldsymbol{\theta}}_{k-1})^T \boldsymbol{\Gamma}^{-1}(\boldsymbol{\theta} - \hat{\boldsymbol{\theta}}_{k-1})\Big] d\tau \\ &= -\frac{1}{2}\int_0^t (2\boldsymbol{\theta} - \hat{\boldsymbol{\theta}}_k - \hat{\boldsymbol{\theta}}_{k-1})^T \boldsymbol{\Gamma}^{-1}(\hat{\boldsymbol{\theta}}_k - \hat{\boldsymbol{\theta}}_{k-1}) d\tau \\ &= -\int_0^t (\boldsymbol{\theta} - \hat{\boldsymbol{\theta}}_k)^T \boldsymbol{\Gamma}^{-1}(\hat{\boldsymbol{\theta}}_k - \hat{\boldsymbol{\theta}}_{k-1}) d\tau \\ &\quad - \frac{1}{2}\int_0^t (\hat{\boldsymbol{\theta}}_k - \hat{\boldsymbol{\theta}}_{k-1})^T \boldsymbol{\Gamma}^{-1}(\hat{\boldsymbol{\theta}}_k - \hat{\boldsymbol{\theta}}_{k-1}) d\tau. \end{aligned} \quad (37)$$

According to (19) and (20), (37) leads to

$$\tilde{R}_k = -\int_0^t \left(\boldsymbol{\theta} - proj_\theta(\hat{\boldsymbol{\theta}}_k^*)\right)^T \boldsymbol{\Gamma}^{-1} \left(proj_\theta(\hat{\boldsymbol{\theta}}_k^*) - \hat{\boldsymbol{\theta}}_k^*\right.$$

$$
\begin{aligned}
&- \boldsymbol{\Gamma}\boldsymbol{\xi}(\boldsymbol{x}_k)\alpha_k)\, d\tau \\
&- \frac{1}{2}\int_0^t (\hat{\boldsymbol{\theta}}_k - \hat{\boldsymbol{\theta}}_{k-1})^T\, \boldsymbol{\Gamma}^{-1}(\hat{\boldsymbol{\theta}}_k - \hat{\boldsymbol{\theta}}_{k-1}) d\tau \\
&= \int_0^t (\boldsymbol{\theta} - proj_\theta(\hat{\boldsymbol{\theta}}_k^*))^T \boldsymbol{\Gamma}^{-1}(\hat{\boldsymbol{\theta}}_k^* - proj_\theta(\hat{\boldsymbol{\theta}}_k^*)) d\tau \\
&+ \int_0^t (\boldsymbol{\theta} - \hat{\boldsymbol{\theta}}_k)^T \boldsymbol{\xi}(\boldsymbol{x}_k)\alpha_k d\tau \\
&- \frac{1}{2}\int_0^t (\hat{\boldsymbol{\theta}}_k - \hat{\boldsymbol{\theta}}_{k-1})^T\, \boldsymbol{\Gamma}^{-1}(\hat{\boldsymbol{\theta}}_k - \hat{\boldsymbol{\theta}}_{k-1}) d\tau. \qquad (38)
\end{aligned}
$$

By means of (27) and (38), one obtains

$$
\begin{aligned}
\tilde{R}_k \le & \int_0^t \tilde{\boldsymbol{\theta}}_k{}^T \boldsymbol{\xi}(\boldsymbol{x}_k)\alpha_k d\tau \\
& - \frac{1}{2}\int_0^t (\hat{\boldsymbol{\theta}}_k - \hat{\boldsymbol{\theta}}_{k-1})^T \boldsymbol{\Gamma}^{-1}(\hat{\boldsymbol{\theta}}_k - \hat{\boldsymbol{\theta}}_{k-1}) d\tau. \qquad (39)
\end{aligned}
$$

Accordingly, the term $Z_k - Z_{k-1}$ in (31) can be rearranged as

$$
\begin{aligned}
\tilde{Z}_k &\triangleq Z_k - Z_{k-1} \\
&= \frac{1}{2\kappa}\int_0^t ((\rho - \hat{\rho}_k)^2 - (\rho - \hat{\rho}_{k-1})^2) d\tau \\
&= -\frac{1}{\kappa}\int_0^t (\rho - \hat{\rho}_k)(\hat{\rho}_k - \hat{\rho}_{k-1}) d\tau \\
&\quad - \frac{1}{2\kappa}\int_0^t (\hat{\rho}_k - \hat{\rho}_{k-1})^2 d\tau. \qquad (40)
\end{aligned}
$$

Based on (23) and (22), (40) becomes

$$
\begin{aligned}
\tilde{Z}_k &= -\frac{1}{\kappa}\int_0^t (\rho - proj_\rho(\hat{\rho}_k^*))(proj_\rho(\hat{\rho}_k^*) - \hat{\rho}_k^* + \kappa|\alpha_k|) d\tau \\
&\quad - \frac{1}{2\kappa}\int_0^t (\hat{\rho}_k - \hat{\rho}_{k-1})^2 d\tau \\
&= \frac{1}{\kappa}\int_0^t (\rho - proj_\rho(\hat{\rho}_k^*))(\hat{\rho}_k^* - proj_\rho(\hat{\rho}_k^*)) d\tau \\
&\quad - \int_0^t \tilde{\rho}_k|\alpha_k| d\tau - \frac{1}{2\kappa}\int_0^t (\hat{\rho}_k - \hat{\rho}_{k-1})^2 d\tau. \qquad (41)
\end{aligned}
$$

By means of (28), (41) becomes

$$
\tilde{Z}_k \le -\int_0^t \tilde{\rho}_k|\alpha_k| d\tau - \frac{1}{2\kappa}\int_0^t (\hat{\rho}_k - \hat{\rho}_{k-1})^2 d\tau. \qquad (42)
$$

Substituting (36), (39), and (42) into (31) and using the fact that $-\beta\alpha_k\varphi_k \le 0$, the difference ΔJ_k becomes negative definite as

$$
\begin{aligned}
\Delta J_k \le & -\int_0^t \beta\alpha_k\varphi_k d\tau - \frac{1}{2\kappa}\int_0^t (\hat{\rho}_k - \hat{\rho}_{k-1})^2 d\tau - Q_{k-1} \\
& - \frac{1}{2}\int_0^t (\hat{\boldsymbol{\theta}}_k - \hat{\boldsymbol{\theta}}_{k-1})^T \boldsymbol{\Gamma}^{-1}(\hat{\boldsymbol{\theta}}_k - \hat{\boldsymbol{\theta}}_{k-1}) d\tau \\
\le & -\int_0^t \beta\alpha_k\varphi_k d\tau - Q_{k-1} \le 0. \qquad (43)
\end{aligned}
$$

Case 2. $T_k < t \le \mathtt{T}$*:* First, analogous to (36), the term Q_k in (31) becomes

$$
Q_k \le \int_0^{T_k} \left[-\alpha_k \tilde{\boldsymbol{\theta}}_k^T \boldsymbol{\xi}(\boldsymbol{x}_k) - \beta\alpha_k\varphi_k + |\alpha_k|\tilde{\rho}_k\right] d\tau. \qquad (44)
$$

Then, analogous to (39) and (42), the terms $\tilde{R}_k$ and $\tilde{Z}_k$ become

$$
\begin{aligned}
\tilde{R}_k \le & \int_0^{T_k} \tilde{\boldsymbol{\theta}}_k{}^T \boldsymbol{\xi}(\boldsymbol{x}_k)\alpha_k d\tau \\
& - \frac{1}{2}\int_0^{T_k} (\hat{\boldsymbol{\theta}}_k - \hat{\boldsymbol{\theta}}_{k-1})^T \boldsymbol{\Gamma}^{-1}(\hat{\boldsymbol{\theta}}_k - \hat{\boldsymbol{\theta}}_{k-1}) d\tau \qquad (45)
\end{aligned}
$$

and

$$
\tilde{Z}_k \le -\int_0^{T_k} \tilde{\rho}_k|\alpha_k| d\tau - \frac{1}{2\kappa}\int_0^{T_k} (\hat{\rho}_k - \hat{\rho}_{k-1})^2 d\tau \qquad (46)
$$

respectively.

Substituting (44)–(46) into (31), for $T_k < t \le \mathtt{T}$, we have

$$
\Delta J_k \le -\int_0^{T_k} \beta\alpha_k\varphi_k d\tau - Q_{k-1} \le 0. \qquad (47)
$$

Then, combining (43) and (47) yields

$$
\Delta J_k \le -\int_0^{\min\{T_k, t\}} \beta\alpha_k\varphi_k d\tau - Q_{k-1} \le 0. \qquad (48)
$$

Part 2. asymptotic and pointwise convergence of $e_{1,k}(t)$ *and* $e_{2,k}(t)$.

According to (43) and (48), we know that J_k is nonincreasing. If J_0 is bounded, then J_k will be bounded. First, we prove the boundedness of J_0. According to (30), with $k = 0$, one has

$$
\begin{aligned}
J_0 = & \frac{k_v^2}{\pi}\tan\left(\frac{\pi\varsigma_0^2(t)}{2k_v^2}\right) + \frac{1}{2}\int_0^t \tilde{\boldsymbol{\theta}}_0{}^T(\tau)\, \boldsymbol{\Gamma}^{-1}\tilde{\boldsymbol{\theta}}_0(\tau) d\tau \\
& + \frac{1}{2\kappa}\int_0^t \tilde{\rho}_0^2(\tau) d\tau. \qquad (49)
\end{aligned}
$$

Here, the cases where $0 \le t \le T_k$ and $T_k < t \le \mathtt{T}$ are also considered separately.

Case 1. $t \le T_k$*:* For this case, according to (29), (30), and (36), the derivative of J_0 is

$$
\begin{aligned}
\dot{J}_0 &= \frac{\varphi_0}{\cos^2(\frac{\pi\varphi_0^2}{2k_v^2})}\dot{\varphi}_0 + \frac{1}{2}\tilde{\boldsymbol{\theta}}_0{}^T \boldsymbol{\Gamma}^{-1}\tilde{\boldsymbol{\theta}}_0 + \frac{1}{2\kappa}\tilde{\rho}_0^2 \\
&\le -\alpha_0 \boldsymbol{\xi}^T(\boldsymbol{x}_0)\tilde{\boldsymbol{\theta}}_0 + |\alpha_0|\tilde{\rho}_0 + \frac{1}{2}\tilde{\boldsymbol{\theta}}_0{}^T \boldsymbol{\Gamma}^{-1}\tilde{\boldsymbol{\theta}}_0 + \frac{1}{2\kappa}\tilde{\rho}_0^2. \qquad (50)
\end{aligned}
$$

By virtue of (20) and (23), (50) yields

$$
\begin{aligned}
\dot{J}_0 \le & (\hat{\boldsymbol{\theta}}_0^* - \hat{\boldsymbol{\theta}}_{-1})^T \boldsymbol{\Gamma}^{-1}\tilde{\boldsymbol{\theta}}_0 + \frac{1}{2}\tilde{\boldsymbol{\theta}}_0{}^T \boldsymbol{\Gamma}^{-1}\tilde{\boldsymbol{\theta}}_0 \\
& + \frac{1}{\kappa}(\hat{\rho}_0^* - \hat{\rho}_{-1})\tilde{\rho}_0 + \frac{1}{2\kappa}\tilde{\rho}_0^2. \qquad (51)
\end{aligned}
$$

Based on (19), (22), and (51), we have

$$
\begin{aligned}
\dot{J}_0 &\le \hat{\boldsymbol{\theta}}_0^{*T}\boldsymbol{\Gamma}^{-1}\tilde{\boldsymbol{\theta}}_0 + \tilde{\boldsymbol{\theta}}_0{}^T \boldsymbol{\Gamma}^{-1}\tilde{\boldsymbol{\theta}}_0 + \frac{1}{\kappa}\hat{\rho}_0^*\tilde{\rho}_0 + \frac{1}{\kappa}\tilde{\rho}_0^2 \\
&= \hat{\boldsymbol{\theta}}_0^{*T}\boldsymbol{\Gamma}^{-1}\tilde{\boldsymbol{\theta}}_0 + (\boldsymbol{\theta} - \hat{\boldsymbol{\theta}}_0)^T \boldsymbol{\Gamma}^{-1}\tilde{\boldsymbol{\theta}}_0 \\
&\quad + \frac{1}{\kappa}\hat{\rho}_0^*\tilde{\rho}_0 + \frac{1}{\kappa}(\rho - \hat{\rho}_0)\tilde{\rho}_0. \qquad (52)
\end{aligned}
$$

By using (27) and (28) of Lemma 1, (52) leads to

$$
\begin{aligned}
\dot{J}_0 &\le (\hat{\boldsymbol{\theta}}_0^* - proj_\theta(\hat{\boldsymbol{\theta}}_0^*))^T\boldsymbol{\Gamma}^{-1}(\boldsymbol{\theta} - proj_\theta(\hat{\boldsymbol{\theta}}_0^*)) + \boldsymbol{\theta}^T \boldsymbol{\Gamma}^{-1}\tilde{\boldsymbol{\theta}}_0 \\
&\quad + \frac{1}{\kappa}(\hat{\rho}_0^* - proj_\rho(\hat{\rho}_0^*))(\rho - proj_\rho(\hat{\rho}_0^*)) + \frac{1}{\kappa}\rho\,\tilde{\rho}_0 \\
&\le \boldsymbol{\theta}^T \boldsymbol{\Gamma}^{-1}\tilde{\boldsymbol{\theta}}_0 + \frac{1}{\kappa}\rho\,\tilde{\rho}_0. \qquad (53)
\end{aligned}
$$

According to Young's inequality, (53) leads to

$$\dot{J}_0 \le c_1\psi_{\max}(\mathbf{\Gamma}^{-1})||\tilde{\boldsymbol{\theta}}_0||^2 + \frac{1}{4c_1}||\boldsymbol{\theta}||^2 + \frac{1}{\kappa}\, c_2|\tilde{\rho}_0|^2 + \frac{1}{4c_2}\rho^2 \tag{54}$$

where c_1, c_2 are positive constants.

Note that $\dot{J}_0$ is bounded since $\tilde{\boldsymbol{\theta}}_0$ and $\tilde{\rho}_0$ are bounded by (25) and (26). As a result, J_0 is continuous such that J_0 is bounded. The boundedness of J_0 and the nonincreasing characteristic of J_k lead to the boundedness of J_k.

Case 2. $T_k < t \le \mathtt{T}$*:* The analysis in the time interval $[0, T_k]$ is analogous to the above case. In the time interval $[T_k, t]$, based on (29), (19)–(21), and (22)–(24), one can obtain

$$\begin{aligned}\dot{J}_0 &\le \frac{1}{2}\tilde{\boldsymbol{\theta}}_0{}^T\mathbf{\Gamma}^{-1}\tilde{\boldsymbol{\theta}}_0 + \frac{1}{2\kappa}\tilde{\rho}_0^2 \\ &= \frac{1}{2}(\boldsymbol{\theta}-\hat{\boldsymbol{\theta}}_{-1})^T\mathbf{\Gamma}^{-1}(\boldsymbol{\theta}-\hat{\boldsymbol{\theta}}_{-1}) + \frac{1}{2\kappa}(\rho-\hat{\rho}_{-1})^2 \\ &= \frac{1}{2}\theta^T\mathbf{\Gamma}^{-1}\boldsymbol{\theta} + \frac{1}{2\kappa}\rho^2. \end{aligned} \tag{55}$$

Therefore, according to the analysis of Case 1 and the fact that $\boldsymbol{\theta}$ and ρ are bounded according to Lemma 1, J_0 is bounded. Next, we prove the convergence of $\varphi_k(t)$. Summing (48) from 1 to k yields

$$\begin{aligned}J_k &\le J_0 - \beta\sum_{j=1}^{k}\int_0^{\min\{T_j,t\}}\alpha_j\varphi_j d\tau - Q_{j-1} \\ &= J_0 - \beta\sum_{j=1}^{k}\int_0^{\min\{T_j,t\}}\alpha_j\varphi_j d\tau \\ &\quad - \sum_{j=1}^{k}\frac{k_v^2}{\pi}\tan\left(\frac{\pi\varsigma_{j-1}^2(t)}{2k_v^2}\right)\end{aligned} \tag{56}$$

and

$$\begin{aligned}\lim_{k\to\infty}J_k &\le J_0 - \beta\lim_{k\to\infty}\sum_{j=1}^{k}\int_0^{\min\{T_j,t\}}\alpha_j\varphi_j d\tau \\ &\quad - \lim_{k\to\infty}\sum_{j=1}^{k}\frac{k_v^2}{\pi}\tan\left(\frac{\pi\varsigma_{j-1}^2(t)}{2k_v^2}\right).\end{aligned} \tag{57}$$

Based on inequality (57), the boundedness of J_0 and J_k implies that the infinite series $\sum_{j=1}^{\infty}\frac{k_v^2}{\pi}\tan(\frac{\pi\varsigma_{j-1}^2}{2k_v^2})$ converges. Hence, $\varsigma_k(t)$ converges to zero asymptotically along the iteration axis for all $t \in [0, \mathtt{T}]$, namely, $\lim_{k\to\infty}\varsigma_k(t) = 0\ \forall t \in [0, \mathtt{T}]$. Note that in the time interval $t \in [0, \mathtt{T}]$, if the actual system error $\varphi_k(t)$ exists, it always satisfies that $\varphi_k(t) = \varsigma_k(t)$. Based on the above discussion, it is straightforward to derive that $\lim_{k\to\infty}\varphi_k(t) = 0 \quad \forall t \in [0, \mathtt{T}]$.

Based on the definition of the extended error $\varphi_k(t)$ in (16), we have

$$\varphi_k = \left(\frac{d}{dt} + \psi_1\right)e_{1,k}. \tag{58}$$

Since $\frac{d}{dt} + \psi_1$ is a stable polynomial, the asymptotic convergence of $\varphi_k(t)\ \forall t \in [0, \mathtt{T}]$ implies the asymptotic convergence of the tracking error $e_{1,k}\ \forall t \in [0, \mathtt{T}]$. Moreover, based on (16), the asymptotic convergence of $s_k(t)$ and $e_{1,k}\ \forall t \in [0, \mathtt{T}]$ implies the asymptotic convergence of $e_{2,k}\ \forall t \in [0, \mathtt{T}]$.

T2) Here, the upper bounds of the position state $s_k(t)$, speed state $v_k(t)$, and input force $u_k(t)$ will be given first. Then, we will prove that all the system constraints can be satisfied. Note that the term $Q_k \triangleq \frac{k_v^2}{\pi}\tan(\frac{\pi\varsigma_k^2}{2k_v^2})$ in J_k goes to infinity as the argument $|\varsigma_k|$ approaches the limit k_v. However, based on T1), J_k is always bounded; hence, $Q_k \triangleq \frac{k_v^2}{\pi}\tan(\frac{\pi\varsigma_k^2}{2k_v^2})$ in J_k is also bounded for any iteration. On the other hand, in the time interval $t \in [0, \mathtt{T}]$, if the actual system error $\varphi_k(t)$ exists, it always satisfies $\varphi_k(t) = \varsigma_k(t)$. Therefore, the boundedness of Q_k and $\varphi_k(0) = 0$ will guarantee that $|\varphi_k| < k_v$ for all time and iterations.

Then, solving the following first-order differential from (16)

$$\dot{e}_{1,k}(t) + \psi_1 e_{1,k}(t) = \varphi_k(t) \tag{59}$$

we will obtain that

$$e_{1,k}(t) = \int_0^t \varphi_k(\tau)e^{-\psi_1(t-\tau)}d\tau + e_{1,k}(0)e^{-\psi_1 t}. \tag{60}$$

Since $|\varphi_k| < k_v$ and $e_{1,k}(0) = 0$, (60) leads to

$$\begin{aligned}|e_{1,k}(t)| &< k_v\int_0^t e^{-\psi_1(t-\tau)}d\tau \\ &= \frac{k_v}{\psi_1}(1-e^{-\psi_1 t}) \le \frac{k_v}{\psi_1}.\end{aligned} \tag{61}$$

Then, based on (59) and (61), one has

$$|e_{2,k}(t)| < \psi_1|e_{1,k}(t)| + |\varphi_k(t)| \le 2k_v. \tag{62}$$

In terms of (13) and (15), since $e_{1,k}(t) = p_1(t) - s_k(t)$ and $e_{2,k}(t) = p_2(t) - v_k(t)$, we have

$$|s_k| < \frac{k_v}{\psi_1} + \eta_1 \tag{63}$$

and

$$|v_k| < 2k_v + \eta_2. \tag{64}$$

According to the triangular inequality and (18), one has

$$\begin{aligned}|F_k(t)| &\le \beta|\varphi_k(t)| + \psi_1|e_{1,k}| + |e_{2,k}| \\ &\quad + \sum_{z=1}^{N+3}\max\{|\theta_{z,\min}|, |\theta_{z,\max}|\}\cdot|\xi_z| + \rho_{\max} \\ &< (\beta+3)k_v + \sum_{z=1}^{N+3}\max\{|\theta_{z,\min}|, |\theta_{z,\max}|\}\cdot|\xi_z| \\ &\quad + \rho_{\max}.\end{aligned} \tag{65}$$

If we want to retain the position state $s_k(t)$, speed state $v_k(t)$, and input force $F_k(t)$ within the state constraints $x_{j,\max}, j = 1, 2$ and input constraint F_{max}, we can select k_v and β to guarantee the following two formulations:

$$\frac{k_v}{\psi_1} + \eta_1 \le x_{1,\max} \tag{66}$$

$$2k_v + \eta_2 \le x_{2,\max} \tag{67}$$

and

$$\begin{aligned}(\beta+3)k_v + \sum_{z=1}^{N+3}\max\{|\theta_{z,\min}|, |\theta_{z,\max}|\}\cdot|\xi_z| \\ + \rho_{\max} \le F_{\max}.\end{aligned} \tag{68}$$

Then, all the system constraints (11), (12) can always be satisfied.

This completes the proof.

Remark 6: In the proposed AFILC (18)–(24), four control parameters β, ψ_1 that appears in both $\varphi_k(t)$ and $\bar{\boldsymbol{\psi}}$, $\boldsymbol{\Gamma}$, κ are needed to be determined before the implementation of the controller. β can be chosen according to (48) and (68). Based on the premise that the inequality (68) is satisfied, β is suggested to be as large as possible. The reason is that a larger value of β will contribute to a more negative term in the right-hand side of (48) such that a faster convergence rate can be expected. ψ_1 can be chosen according to (61). The larger ψ_1 is, the smaller the tracking error will be. In like manner, according to (43), the smaller $\boldsymbol{\Gamma}$ and κ are, the faster the convergence rate will be. In addition, other design parameters k_v, $\boldsymbol{\theta}_{\min}$, $\boldsymbol{\theta}_{\max}$, $\rho_{\min}$, $\rho_{\max}$, $\boldsymbol{x}_{\max}$ can be prespecified for different systems, based on the knowledge of system specifications or certain hardware limits of the real plant.

Remark 7: In practice, a HST should always run under both the speed constraint $v_{\max}$ and input force constraint $F_{\max}$ to ensure safety. According to (64) and (65) in the proof of Theorem 1, the proposed AFILC (18)–(24) can always keep the actual speed and input force below $2k_v + \eta_2$ and $(\beta+3)k_v + \sum_{z=1}^{N+3} \max\{|\theta_{z,\min}|, |\theta_{z,\max}|\} \cdot |\xi_z|$, respectively. Moreover, selecting the control parameters based on the provided guidance in Remark 6 to make the inequalities $2k_v + \eta_2 \leq v_{\max}$ and $(\beta+3)k_v + \sum_{z=1}^{N+3} \max\{|\theta_{z,\min}|, |\theta_{z,\max}|\} \cdot |\xi_z| + \rho_{\max} \leq F_{\max}$ hold, then the proposed AFILC can always make the train actively and automatically run under both the speed and input force constraints.

Remark 8: The identical desired trajectory in each iteration of the system is a common assumption in the traditional ILC methods, and it can be easily relaxed to be iteration-varying one in the context of adaptive ILC [41]. In practical operation of the HST, if the desired position and speed trajectories are changed on different days, the proposed AFILC can also learn from these iteration-varying trajectories and guarantee the convergence property.

IV. Simulation Study

A train operation system similar to Chinese electric multiple-unit HST CRH-3 is simulated here.

In the simulation, the railway track is 52.3 km in total. Note that in practical operation, a train is always subject to various unknown external disturbances such as the load disturbance caused by different numbers of passengers between weekdays and weekends or between different stations, and the unknown temperature changes in different seasons, etc. To show the robustness of the proposed method against these unknown external disturbances, $d_k(t)$ in the dynamic model (1) is set to be randomly and iteratively varying within $[-7, 7]/\mathtt{M}$ (kN/kg), where $\mathtt{M} = 350\,000$ (kg) is the nominal mass of the train. In the simulation, the train repetitively tracks the desired position and speed trajectories 100 times for the passenger transportation task. The expected iteration length is $\mathtt{T} = 2500$ (s), and the actual iteration length T_k varies randomly over the time interval $[2400, 2600]$ (s), as shown in Fig. 2.

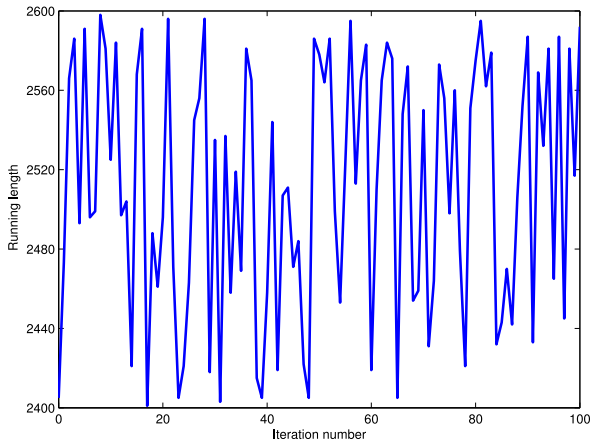

Fig. 2. Running length of each iteration.

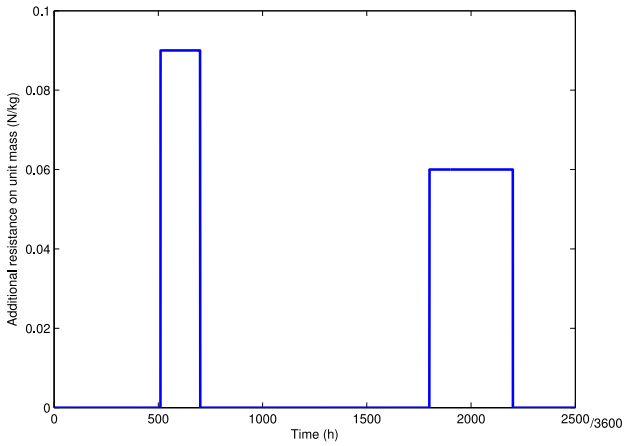

Fig. 3. Additional resistance on a unit mass along the track.

The actual basic resistance coefficients $a(t)$, $b(t)$ and $c(t)$ in (2) satisfy

$$\begin{aligned} a(t) &= [2977 + 275\,\sin(0.0037t)]/\mathtt{M} \\ b(t) &= [25.17 + 2.4\,\sin(0.0037t)]/\mathtt{M} \\ c(t) &= (0.3864 + 0.04\,\sin(0.0037t))/\mathtt{M} \end{aligned} \tag{69}$$

where $a(t)$ denotes the rolling resistance coefficient, $b(t)$ is associated with a drag coefficient caused by friction and train vibration, and $c(t)$ is the aerodynamic resistance coefficient. In the simulation, these time-varying basic resistance coefficients are all unknown and are estimated and compensated by the proposed AFILC (18)–(24).

Note that if the HST can strictly run over the fixed time interval [0, 2500] (s) for each operation, the additional resistance $f_a(s_k(t))$ in (1) can be described as shown in Fig. 3. However, since the actual running length varies over the time interval $[2400, 2600]$ (s), as shown in Fig. 2, the actual additional resistance $f_a(s_k(t))$ in the train's dynamics will be randomly varying according to each operation. The $f_a(s_k(t))$ values at the 4th, 40th, and 80th iterations are shown in Fig. 4. In the simulation, this iteratively varying additional resistance $f_a(s_k(t))$

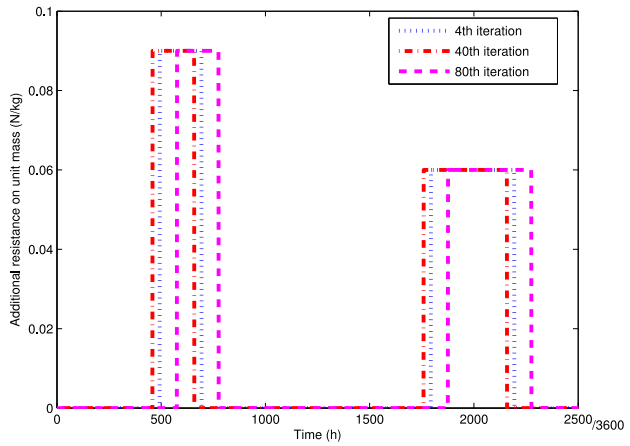

Fig. 4. Additional resistance on a unit mass along the track at the 4th, 40th, and 80th iterations.

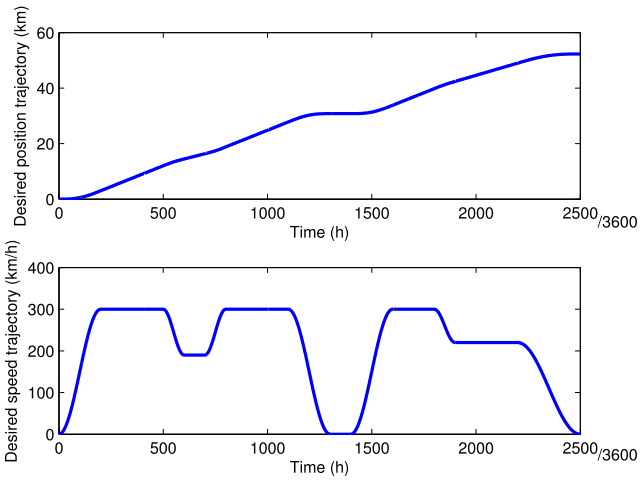

Fig. 5. Desired speed and position trajectories.

is completely unknown and is estimated by the constructed fuzzy learning system (3)–(8) and compensated by the proposed AFILC (18)–(24).

The train operates at the desired speed under 300 (km/h) along the entire track. The desired position $p_1(t)$ and speed $p_2(t)$ defined in (13) are shown in Fig. 5.

In Chinese Train Control System Level 3 (CTCS-3), the speed tolerance of the CTCS-3 onboard equipment to trigger an alarm is 2 km/h [42]. Accordingly, in the simulation, the speed constraint is set if the actual speed of the train exceeds the desired speed by 2 km/h, as shown in Figs. 8–9. In addition, according to the traction characteristic curve of CRH-3 [43], the maximum traction force under 300 (km/h) approximately satisfies

$$F_{\max}(kN) = \begin{cases} 300 - 0.284v_k & v_k \le 119.7(\text{km/h}) \\ 266 \times 119.7/v_k & 119.7 < v_k \le 300(\text{km/h}). \end{cases} \tag{70}$$

The objective of the simulation is to make the actual $s_k(t)$ and $v_k(t)$ track the desired $p_1(t)$ and $p_2(t)$ over the whole expected time interval [0, 2500] (s), even if the actual time

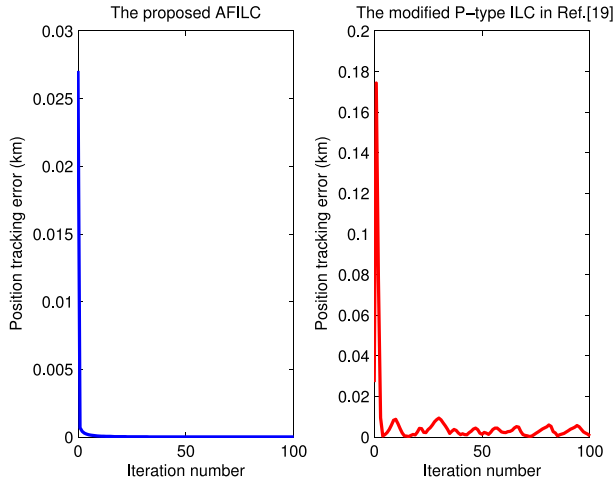

Fig. 6. Position tracking errors.

interval varies randomly in $[2400, 2600]$ (s); meanwhile, all the system constraints are always satisfied.

For comparison, the modified P-type ILC for HSTs with varying operation lengths in Yu *et al.* [19] is also simulated.

A. Proposed AFILC With Varying Iteration Lengths and System Constraints

The proposed learning control law (18) and (19)–(24) is simulated, and the control parameters are selected as $\beta = 0.5$, $\bar{\boldsymbol{\psi}} = [0,\ 1]^T$, $\boldsymbol{\Gamma} = \text{diag}\{10^{-5}, 10^{-5}, 10^{-5}, 10^{-4}, 10^{-4}, 10^{-4}, 10^{-4}\}$, $\kappa = 10^{-4}$, $k_v = 1$, and $\hat{\boldsymbol{\theta}}_k(0) = [0, 0, 0, 0, 0, 0, 0\ ]^T$. By means of (3)–(8) for the estimation of the unknown nonlinear function $f_a(s_k(t))$, four fuzzy rules are designed with the following centers and the widths $m_1^1(t) = -3 * p_1(t)$, $m_2^1(t) = -3 * p_2(t)$; $m_1^2(t) = p_1(t)$, $m_2^2(t) = p_2(t)$; $m_1^3(t) = -p_1(t)$, $m_2^3(t) = -p_2(t)$; $m_1^4(t) = 2 * p_1(t)$, $m_2^4(t) = 2 * p_2(t)$; $\sigma_1^l(t) = 50$, $\sigma_2^l(t) = 50$; $\sigma_1^2(t) = 30$, $\sigma_2^2(t) = 30$; $\sigma_1^3(t) = 35$, $\sigma_2^3(t) = 35$; $\sigma_1^4(t) = 40$, $\sigma_2^4(t) = 40$.

B. Modified P-Type ILC in Yu et al. [19]

Here, the modified P-type ILC for HSTs with varying operation lengths in Yu *et al.* [19] is simulated for comparison

$$u_{k+1}(t) = u_k(t) + \boldsymbol{K}\boldsymbol{e}_k^{\phi}(t) \tag{71}$$

where if $T_k < \mathtt{T}$

$$\boldsymbol{e}_k^{\phi}(t) = \begin{cases} \boldsymbol{e}_k(t), & 0 \le t \le T_k \\ 0, & T_k + 1 < t \le \mathtt{T} \end{cases} \tag{72}$$

if $T_k \ge \mathtt{T}$

$$\boldsymbol{e}_k^{\phi}(t) = \boldsymbol{e}_k(t) \quad 0 \le t \le \mathtt{T} \tag{73}$$

$\boldsymbol{K} = [K_1\ , K_2]$ is a learning gain vector. By means of intensive tuning, the values $K_1 = 0.002$ and $K_2 = 0.002$ are selected.

The simulation results of these two methods are shown in Figs. 6–9.

Figs. 6 and 7 demonstrate the tracking control performance of these two methods in 100 repetitive operations. Here, the root mean square (RMS) of the tracking errors over the whole actual operating time interval is used to evaluate the control

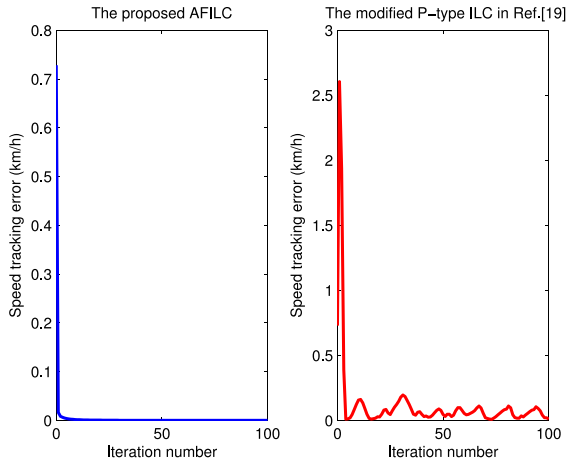

Fig. 7. Speed tracking errors.

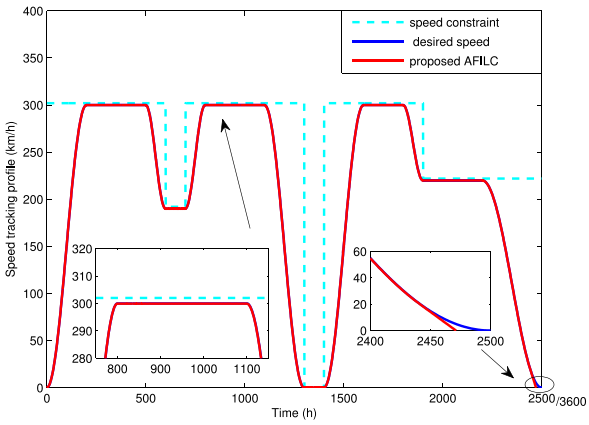

Fig. 8. Speed tracking profile of the proposed AFILC at the first iteration.

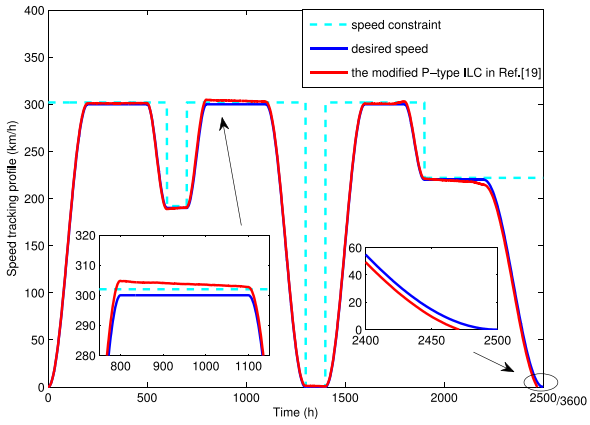

Fig. 9. Speed tracking profile of the modified P-type ILC in Yu *et al.* [19] at the first iteration.

performance. As shown in Figs. 6 and 7, the proposed method gradually reduces both the position and speed errors of the train as the number of iterations increases, even if the system is subject to the randomly varying iteration length and unknown external disturbances. However, when applying the modified P-type ILC, undesirable transient behavior is observed in both the position and speed errors, which results in unsafe operation of the HST.

To further illustrate the tracking performance, the speed tracking profiles of the two methods at the first iteration are shown in Figs. 8 and 9, where the iteration length of the first iteration is 2473 s. In Figs. 8 and 9, the operation speed of the train when applying the modified P-type ILC exceeded the speed constraint, which would lead to unsafe operation of the train. By contrast, the proposed AFILC ensures that the actual operation speed is always less than the speed constraint, despite the randomly varying iteration length in each operation, while simultaneously satisfying the tracking performance.

V. Conclusion

In this article, a new AFILC was proposed for repetitive nonlinear HST operation systems where both the operating speed and control input force were constrained and the actual iteration length in each operation of the train was randomly varying. A new adaptive iterative learning fuzzy system was constructed to approximate and compensate the nonparametric and unknown additional resistance in the HST operation system. By introducing a BCEF and a newly designed projection mechanism into the designed AFILC, both the system constraints and randomly varying operation lengths could be addressed. Theoretical analysis demonstrated that the convergence of the tracking control errors could be guaranteed over the whole desired iteration length, even if the actual iteration length varied in each operation of the HST. Moreover, both the states and the control input of the HST operation system could always be maintained within their constrained bounds for the safe train operation. Simulation results on a practical train operation system similar to the Chinese HST CRH-3 further demonstrated the effectiveness of the proposed method. For further research, it is of interest to investigate coordinated and fault-tolerant AFILC for multiple-train trajectory tracking with randomly varying iteration lengths, system constraints, and traction/braking faults all together.

References

[1] S. Arimoto, S. Kawamura, and F. Miyazaki, "Bettering operation of robots by learning," *J. Robot. Syst.*, vol. 1, no. 2, pp. 123–140, 1984.

[2] H. R. Dong, S. G. Gao, B. Ning, and L. L, "Extended fuzzy logic controller for high speed train," *Neural Comput. Appl.*, vol. 22, no. 2, pp. 321–328, 2013.

[3] H. Yang, K.-P. Zhang, and H.-E. Liu, "Online regulation of high speed train trajectory control based on T-S fuzzy bilinear model," *IEEE Trans. Intell. Transp. Syst.*, vol. 17, no. 6, pp. 1496–1508, Jun. 2016.

[4] Y. D. Song, Q. Song, and W. C. Cai, "Fault-tolerant adaptive control of high speed trains under traction/braking failures: A virtual parameter based approach," *IEEE Trans. Intell. Transp. Syst.*, vol. 15, no. 2, pp. 737–748, Apr. 2014.

[5] K. P. Zhang, B. Jiang, G. Tao, and F. Y. Chen, "MIMO evolution model-based coupled fault estimation and adaptive control with high-speed train applications," *IEEE Trans. Control Syst. Technol.*, vol. 26, no. 5, pp. 1552–1566, Sep. 2018.

[6] K. Ichikawa, "Application of optimization theory for bounded state variable problems to the operation of train," *Bull. JSME*, vol. 11, no. 47, pp. 857–865, 1968.

[7] X. Zhuan and X. H. Xia, "Optimal scheduling and control of heavy haul trains equipped with electronically controlled pneumatic braking systems," *IEEE Trans. Control Syst. Technol.*, vol. 8, no. 4, pp. 855–864, Oct. 2011.

[8] H. B. Ye and R. H. Liu, "Nonlinear programming methods based on closed-form expressions for optimal train control," *Transp. Res. C*, vol. 82, pp. 102–123, 2017.

[9] Y. K. Wu, B. Jiang, and N. Y. Lu, "A descriptor system approach for estimation of incipient faults with application to high-speed railway traction devices," *IEEE Trans. Syst. Man Cybern., Syst.*, vol. 49, no. 10, pp. 2108–2118, Oct. 2019.
[10] Z. H. Mao, G. Tao, B. Jiang, and X.-G. Yan, "Adaptive actuator compensation of position tracking for high-speed trains with disturbances," *IEEE Trans. Veh. Technol.*, vol. 67, no. 7, pp. 5706–5717, Jul. 2018.
[11] Z. X. Li and Z. S. Hou, "Adaptive iterative learning control based high speed train operation tracking under iteration-varying parameter and measurement noise," *Asian J. Control*, vol. 17, no. 5, pp. 1779–1788, 2015.
[12] Q. X. Yu, Z. S. Hou, and R. H. Chi, "Adaptive iterative learning control for nonlinear uncertain systems with both state and input constraints," *J. Franklin Inst.*, vol. 353, pp. 3920–3943, 2016.
[13] H. H. Ji, Z. S. Hou, and R. K. Zhang, "Adaptive iterative learning control for high-speed trains with unknown speed delays and input saturations," *IEEE Trans. Autom. Sci. Eng.*, vol. 13, no. 1, pp. 260–273, Jan. 2016.
[14] H. H. Ji, Z. S. Hou, L. L. Fan, and F. L. Lewis, "Adaptive iterative learning reliable control for a class of non-linearly parameterised systems with unknown state delays and input saturation," *IET Control Theory Appl.*, vol. 10, no. 17, pp. 2160–2174, 2016.
[15] W. J. Davis, "Traction resistance of electric locomotives and cars," *General Elect. Rev.*, vol. 29, no. 10, pp. 685–708, 1926.
[16] W. W. Hay, *Railroad Engineering*. 2nd ed. New York, NY, USA: Wiley, 1982.
[17] H. Q. Sun, Z. S. Hou, and D. Y. Li, "Coordinated iterative learning control schemes for train trajectory tracking with overspeed protection," *IEEE Trans. Autom. Sci. Eng.*, vol. 10, no. 2, pp. 323–333, Apr. 2013.
[18] Q. X. Yu, Z. S. Hou, and J.-X. Xu, "D-type ILC based dynamic modeling and norm optimal ILC for high-speed trains," *IEEE Trans. Control Syst. Technol.*, vol. 26, no. 2, pp. 652–663, Mar. 2018.
[19] Q. X. Yu, X. H. Bu, R. H. Chi, and Z. S. Hou, "Modified P-type ILC for high-speed trains with varying trial lengths," in *Proc. IEEE 7th Data Driven Control Learn. Syst. Conf.*, Eenshi, China, 2018, pp. 1006–1010.
[20] X. F. Li, J.-X. Xu, and D. Q. Huang, "An iterative learning control approach for linear systems with randomly varying trial lengths," *IEEE Trans. Autom. Control*, vol. 59, no. 7, pp. 1954–1960, Jul. 2014.
[21] D. Shen, W. Zhang, Y. Q. Wang, and C. J. Chien, "On almost sure and mean square convergence of P-type ILC under randomly varying iteration lengths," *Automatica*, vol. 63, pp. 359–365, 2016.
[22] X. F. Li and D. Shen, "Two novel iterative learning control schemes for systems with randomly varying trial lengths," *Syst. Control Lett.*, vol. 107, pp. 9–16, 2017.
[23] J. T. Shi, X. He, and D. H. Zhou, "Iterative learning control for nonlinear stochastic systems with variable pass length," *J. Franklin Inst.*, vol. 353, pp. 4016–4038, 2016.
[24] X. H. Bu, S. Wang, Z. S. Hou, and W. Liu, "Model free adaptive iterative learning control for a class of nonlinear systems with randomly varying iteration lengths," *J. Franklin Inst.*, vol. 356, pp. 2491–2504, 2019.
[25] D. Shen and J.-X. Xu, "Adaptive learning control for nonlinear systems with randomly varying iteration lengths," *IEEE Trans. Neural Netw.*, vol. 30, no. 4, pp. 1119–1132, Apr. 2019.
[26] J. H. Zhang, P. Shi, and Y. Q. Xia, "Robust adaptive sliding-mode control for fuzzy systems with mismatched uncertainties," *IEEE Trans. Fuzzy Syst.*, vol. 18, no. 4, pp. 700–711, Aug. 2010.
[27] S. C. Tong, T. Wang, and Y. M. Li, "Fuzzy adaptive actuator failure compensation control of uncertain stochastic nonlinear systems with unmodeled dynamics," *IEEE Trans. Fuzzy Syst.*, vol. 22, no. 3, pp. 563–574, Jun. 2014.
[28] K. K. Sun, S. S. Mou, J. B. Qiu, T. Wang, and H. J. Gao, "Adaptive fuzzy control for nontriangular structural stochastic switched nonlinear systems with full state constraints," *IEEE Trans. Fuzzy Syst.*, vol. 27, no. 8, pp. 1587–1601, Aug. 2019.
[29] A. Q. Wang, L. Liu, J. B. Qiu, and G. Feng, "Event-triggered robust adaptive fuzzy control for a class of nonlinear systems," *IEEE Trans. Fuzzy Syst.*, vol. 27, no. 8, pp. 1648–1658, Aug. 2019.
[30] A. Chibani, M. Chadli, S. X. Ding, and N. B. Braiek, "Design of robust fuzzy fault detection filter for polynomial fuzzy systems with new finite frequency specifications," *Automatica*, vol. 93, pp. 42–54, 2018.
[31] R. E. Precup, M. L. Tomescu, and C. A. Dragos, "Stabilization of Rössler chaotic dynamical system using fuzzy logic control algorithm," *Int. J. General Syst.*, vol. 43, no. 5, pp. 413–433, 2014.
[32] X. Wang, S. K. Li, S. Su, and T. Tang, "Robust fuzzy predictive control for automatic train regulation in high-frequency metro lines," *IEEE Trans. Fuzzy Syst.*, vol. 27, no. 6, pp. 1295–1308, Jun. 2019.
[33] S. N. Givigi, H. M. Schwartz, and X. S. Lu, "A reinforcement learning adaptive fuzzy controller for differential games," *J. Intell. Robot. Syst.*, vol. 59, no. 1, pp. 3–30, 2010.
[34] R. P. A. Gil, Z. C. Johanyák, and T. Kovács, "Surrogate model based optimization of traffic lights cycles and green period ratios using microscopic simulation and fuzzy rule interpolation," *Int. J. Artif. Intell*, vol. 16, no. 1, pp. 20–40, 2018.
[35] R. S. Raghunathan, H. D. Kim, and T. Setoguchi, "Aerodynamics of high-speed railway train," *Progr. Aerosp. Sci.*, vol. 38, no. 6-7, pp. 469–514, Aug.–Oct. 2002.
[36] L. X. Wang, "Stable adaptive fuzzy control of nonlinear systems," *IEEE Trans. Fuzzy Syst.*, vol. 1, no. 2, pp. 146–155, May 1993.
[37] Z. S. Hou, J.-X. Xu, and J. W. Yan, "An iterative learning approach for density control of freeway traffic flow via ramp metering," *Transp. Res. C*, vol. 16, no. 1, pp. 71–97, Feb. 2008.
[38] X. Li, Y. H. Liu, and H. Yu, "Iterative learning impedance control for rehabilitation robots driven by series elastic actuators," *Automatica*, vol. 90, pp. 1–7, 2018.
[39] Y. Hui, R. H. Chi, B. Huang, and Z. S. Hou, "Extended state observer-based data-driven iterative learning control for permanent magnet linear motor with initial shifts and disturbances," *IEEE Trans. Syst. Man Cybern., Syst.*, to be published, doi: 10.1109/TSMC.2019.2907379.
[40] M. X. Sun and S. S. Ge, "Adaptive repetitive control for a class of nonlinearly parametrized systems," *IEEE Trans. Autom. Control*, vol. 51, no. 10, pp. 1684–1688, Oct. 2006.
[41] J. X. Xu and J. Xu, "On iterative learning from different tracking tasks in the presence of time-varying uncertainties," *IEEE Trans. Syst., Man, Cybern., Part B, Cybern.*, vol. 34, no. 1, pp. 589–597, Feb. 2004.
[42] J. F. Wang, Y. J. Li, and Y. Zhang, "Research on parallel control mechanism and its implementation in ATP," *IEEE Trans. Intell. Transp. Syst.*, vol. 17, no. 6, pp. 1652–1662, Jun. 2016.
[43] L. Li, W. Dong, Y. D. Ji, Z. K. Zhang, and L. Tong, "Minimal-energy driving strategy for high-speed electric train with hybrid system model," *IEEE Trans. Intell. Transp. Syst.*, vol. 14, no. 4, pp. 1642–1653, Dec. 2013.

Qiongxia Yu received the B.S. degree in electrical engineering and automation, and the M.S. degree in control theory and control engineering, from Henan Polytechnic University, Jiaozuo, China, in 2009 and 2012, respectively, and the Ph.D. degree in control theory and control engineering from Beijing Jiaotong University, Beijing, China, in 2017.

She is currently a Lecturer with Henan Polytechnic University. Her current research interests include learning control, fuzzy control, data-driven control and their applications in transportation systems.

Zhongsheng Hou (Fellow, IEEE) received the Ph.D. degree in control science and engineering from Northeastern University, Shenyang, China, in 1994.

He was a Postdoctoral Fellow with Harbin Institute of Technology, China, from 1995 to 1997, and a Visiting Scholar at Yale University, New Haven, CT, USA, from 2002 to 2003. From 1997 to 2018, he was with Jiaotong University, Beijing, China, where he was a Distinguished Professor and Founding Director of Advanced Control Systems Lab, and Head of Department of Automatic Control. Currently, he is a Chair Professor with the School of Automation, Qingdao University, Qingdao, China. He has published more than 180 peer-reviewed journal papers and more than 140 papers in prestigious conference proceedings. His current research interests include the fields of data-driven control, model-free adaptive control, learning control, and intelligent transportation systems.

Prof. Hou's pioneering contributions in data driven control and learning control have been recognized by multiple projects supported by the National Natural Science Foundation of China (NSFC), including three key projects of NSFC, 2009, 2015, and 2019, respectively, and a major international cooperation project of NSFC, 2012, and by his leading role as a Guest Editor in two Special Sections on the topic of data-driven control in the IEEE TRANSACTIONS ON NEURAL NETWORKS, 2011, and the IEEE TRANSACTIONS ON INDUSTRIAL ELECTRONICS, 2017.